ELSEVIER

Thermal degradation studies of cyclic olefin copolymers

Chenyang Liu, Jian Yu, Xinghua Sun, Jun Zhang, Jiasong He*

State Key Laboratory of Engineering Plastics, Center for Molecular Science, Institute of Chemistry,
The Chinese Academy of Sciences, Beijing 100080, China

Abstract

The influences of the chemical composition and microstructure on the degradation behaviors of 3-series cyclic olefin copolymers (COCs) were investigated by using non-isothermal thermogravimetric analysis (TGA). Kinetic parameters of degradation were evaluated by using the Flynn–Wall–Ozawa iso-conversional method and the pseudo first-order method. Compared with conventional polyolefins, e.g. HDPE, COCs have lower peak temperatures of degradation, narrower degradation temperature ranges and higher amount of residual weights at the end of the degradation, which should be attributed to the chemical structure and microstructure features of COCs including the branching effect and the steric effect. The values of the reaction order of COCs determined by the Kissinger method are close to 1 in the non-isothermal degradation process. Although the values of E_a in region II calculated by using the pseudo first-order method are much higher than those calculated by using the Flynn–Wall–Ozawa method, there is a similar change trend of E_a between these two methods. However, there is a good correlation between the E_a in region II and the peak temperature of degradation for COCs. The theoretical weight loss versus temperature curves, generated by using the estimated kinetic parameters, well fit the experimental data, which indicates that the analysis method used in this work is valid.
© 2003 Elsevier Science Ltd. All rights reserved.

Keywords: Cyclic olefin copolymers (COCs); Thermogravimetric analysis; Thermal stability; Kinetics of degradation

1. Introduction

Cyclic olefin copolymers (COCs) obtained with metallocene catalysts are engineering thermoplastics with some unique properties, such as high glass transition temperatures in combination with excellent transparency, low dielectric loss, low moisture absorption, and good chemical resistance for high-performance optical, medical, electrical, packaging and other applications owing to their rigid cyclic monomer units [1,2]. Since the first report on the synthesis of COCs in 1991 [3], the synthesis of COCs has been the subject of a large number of groups [4,5]. In recent years, it was the focus of the synthesis and characterization of COCs to determine the comonomer composition and sequence distribution along the copolymer chains by ^{13}C NMR spectroscopy [6–10]. The design of COC materials requires a detailed description of the relationships between the micro-structures of copolymers and the metallocene catalysts

used as well as a complete understanding of the relationships between the microstructure and the material properties.

Recently, a wide investigation of physical properties of these COCs is being carried out. The possible relationships among copolymers composition, microstructure and thermal properties have been reported [10–15]. The most common one is a linear relationship between cyclic structure content and T_g for the COCs having similar microstructure or being synthesized by the same metallocene catalyst. Forsyth et al. also studied the stress–strain behavior, microhardness and dynamic mechanical properties of COCs [14,16]. Chu et al. showed phenomenal increase of T_g upon annealing for their series of COCs [17,18], which was attributed to the conformational conversion and local packing of these copolymers. Dorkenoo et al. studied the gas transport properties of a series of high T_g poly-norbornenes with aliphatic pendent groups, and investigated the physical aging process of amorphous films made from these polymers [19,20]. Khanarian studied the optical properties of COCs, and rubber-toughened and optically transparent blends of COCs [21,22].

* Corresponding author. Tel.: +86-010-6261-3251; fax: +86-010-6255-9373.

*E-mail address:* hejs@sklep.icas.ac.cn (J. He).

Miscibility behavior of binary blends of two cyclic olefin copolymers was studied by Delfolie et al. [23]. Their experimental data were compared with theoretical analysis in order to determine how the size and stiffness disparities between the ethylene and norbornene monomers and monomer sequence distribution affect the miscibility patterns. The elongational flow birefringence of ethylene–norbornene copolymer and ethylene–tetracyclododecene copolymer had been performed by Maiti et al. [24,25]. Takigawa et al. studied the influence of rigid comonomer incorporated in copolymers on the rheological properties [26]. However, there remains no systematic study of the effects of composition and microstructure on the long-term performance and degradation behavior of the COCs. It is worthwhile to study the thermal degradation of these semicommercial copolymers which have immense applications.

There are several types of cyclic olefin copolymers based on different types of comonomers [27]. The COCs samples in this study were a collection of IUPAC WP IV.2.1 for international joint research on structure and properties of commercial polymers (No. 421/38/00: "Structure and properties of cyclic olefin copolymers"). Objective of this project is to evaluate the structure–property correlations between the chemical structure and rheological and physical properties of the cyclic olefin copolymers [28]. In a prior study, the chemical structure and microstructure, and correlations between the structure and thermal and rheological properties were presented [15,26]. This study is concerned with the degradation behavior of three-series cyclic olefin copolymers using non-isothermal thermogravimetric analysis. In the present research, we will focus on the influences of the chemical composition and microstructure on the degradation temperatures and the degradation kinetic parameters.

2. Experimental

2.1. Materials

The A, B, and C series cyclic olefin copolymers were supplied by Hoechst Celanese, Mitsui Chemical, Nippon Zeon Co., and Japan Synthetic Rubber, respectively [1,2]. The chemical structures of three-series cyclic olefin copolymers are shown in Scheme 1. The cyclic structure content of these copolymers was determined by ^{13}C NMR spectroscopy and the glass transition temperature T_g was determined by differential scanning calorimetry. The chemical structure and microstructure of the three-series COCs have been studied in detail in prior paper [15]. Table 1 summarizes the characteristics of these copolymers, together with the data of molecular weight, molecular weight distribution and density. HDPE (grade 2480, supplied by Qilu Petrochemical
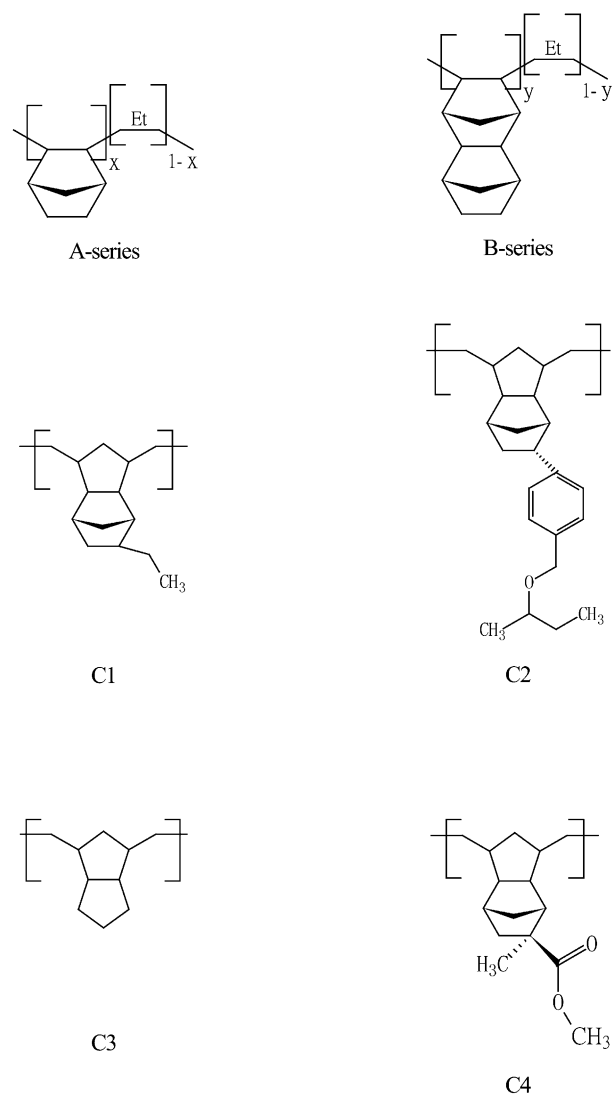
Scheme 1. The chemical structure of cyclic olefin copolymers.

Table 1
Characteristics of these cyclic olefin copolymers studied [15]

Sample	Cyclic structure content (mol%)	Glass transition temperature, T_g (°C)	$M_w \times 10^{-4}$	M_w/M_n	Density (g/cm³)
A1	30.7	84			1.02
A2	41.5	149	9.5	1.79	1.02
A3	45.2	163	9.5	1.77	1.02
A4	58.6	177	9.1	1.91	1.02
B1	20.2	80	8.1	2.52	1.02
B2	27.7	125	8.8	2.59	1.04
B3	31.7	145	10.2	2.68	1.04
C1	50	138	5.8	3.02	1.01
C2	50	139	6.5	1.96	1.01
C3	50	105	4.1	1.55	1.00
C4	50	171			1.08
HDPE					0.94

Corporation of China) was employed as a reference for the study of the thermal degradation for COCs. All samples were used as received.

2.2. TGA measurements

The non-isothermal kinetics of degradation was performed on Perkin-Elmer TGA-7. The thermal analyzer was temperature calibrated between experiments using the Curie point of nickel as a reference. All experiments were carried out under a nitrogen atmosphere at a purge rate of 50 ml/min. For each polymer, samples of approximately 2.5 mg was temperature-equilibrated to 250 °C before being heated to 550 °C at different heating rates (2, 5 and 10 °C/min).

3. Results and discussion

3.1. Thermal stability

The thermogravimetric (TG) and derivative thermogravimetric (DTG) curves for the three-series COCs and

HDPE performed at a constant heating rate of 2 °C/min are shown in Figs. 1–3. For each sample, the thermogram reveals that the DTG plot shows a maximum rate of weight loss, so the peak temperatures of degradation (T_p) can be determined. The onset temperatures of degradation (T_{onset}) can be calculated from the TG curves by extrapolating from the curve at the peak of degradation back to the initial weight of the polymer. Similarly, the end temperature of degradation can be calculated from the TGA curves by extrapolating from the curve at the peak of degradation forward to the final weight of the polymer. These characteristic temperatures are listed in Table 2. The difference of the peak temperatures and the onset temperatures of degradation is ΔT, which represents the temperature range of thermal degradation. As a reference, the data of thermodegradation of HDPE are also listed in Table 2.

On the basis of the experimental results, it can be seen that COCs have maintained the superior thermal stability of polyolefin materials, but the thermal degradations of cyclic olefin copolymers show a different behavior from that of HDPE as follows:
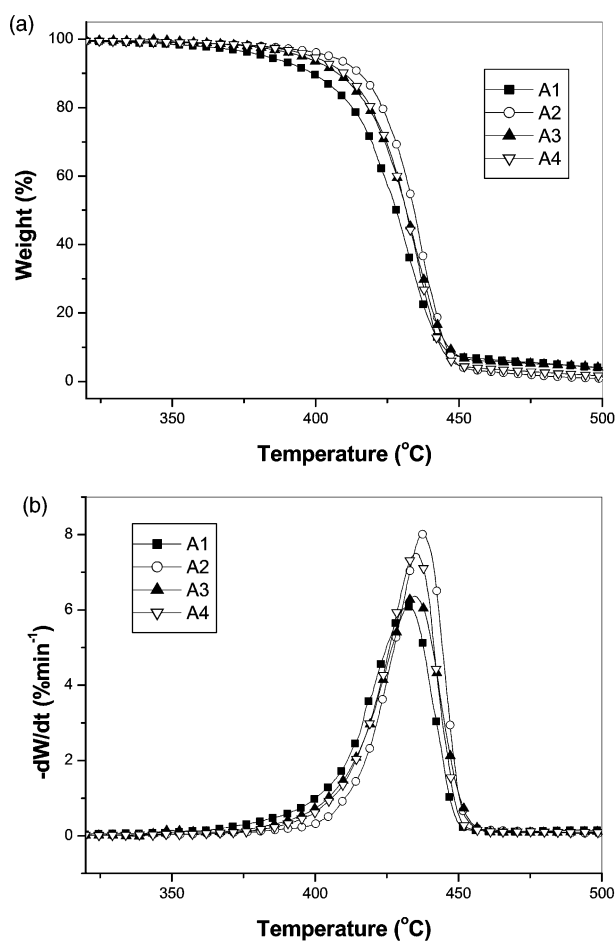

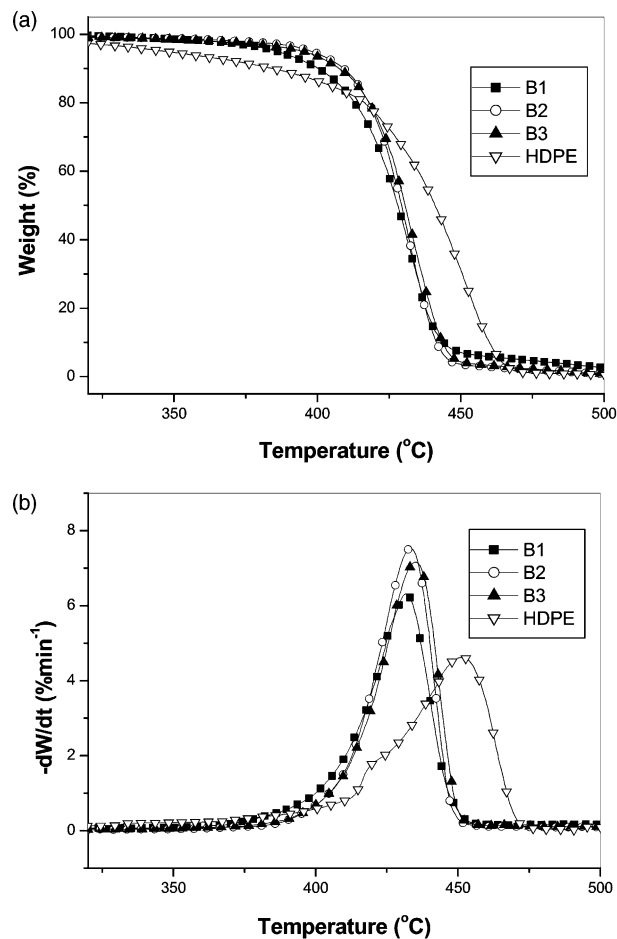Fig. 1. The TGA curves (a) and DTG curves (b) of A-series COCs samples at heating rate 2 °C/min.

Fig. 2. The TGA curves (a) and DTG curves (b) of B-series COCs samples and HDPE at heating rate 2 °C/min.

(a) The onset and peak temperatures of degradation for COCs were lower than those for HDPE, and scattered at about 410 and 430 °C, respectively. It should be attributed to the chemical structure and microstructure features of COCs including the branching effect and the steric effect. Westerhout et al. [29] reviewed the influence of the extent of branching of the main polymer chain on the reaction rate at a given temperature, and found the reaction rate increases with the extent of branching in the following order: HDPE $<$LDPE $<$PP $<$PS, which is identical with the order that the ability of substituents to stabilize macroradicals forming in chain scission (CH$_3$ $<$CH$_2$CH$_3$ $<$CH(CH$_3$)$_2$ $<$C(CH$_3$)$_3$ $<$benzyl, [30]). Gamlin et al. systematically studied the effect of ethylene/propylene content on the thermal degradation behavior of EPDM [31]. They found that both the onset and peak degradation temperatures linearly increased as the ethylene content increases above 40%. However, in this study it appears that the onset and peak degradation temperatures are respectively about 415±4 and 433±2 °C for A- and B-series copolymers except A2 of T_p value 438 °C, although there are larger change on the cyclic structure content and the T_g for these two series samples.

For C-series copolymers, there are larger differences in the side substituents and/or the cyclic structure, which lead to that the onset temperature and peak degradation temperatures are different. It seems that the chemical structure and microstructure features may be playing an important role in determining the degradation temperature. On the one hand, the branching of cyclic structure increases the reaction rate, on the other hand the chain stiffness of cyclic structure reduces the mobility of the chain, then decreases the reaction rate and improves thermal stability [32]. It is interesting to note that both C2 and C4 have lower T_p values 424 °C, but C3 has higher T_p value 440 °C, respectively. There are phenyl groups and ester groups on the side chain of C2 and C4, respectively. Their electron-withdrawing groups stabilize these macroradicals and, therefore, the corresponding samples are less stable [33,34]. Contrarily, compared with other samples of C-series COCs, C3 is absent both the side-group and the rigid bridge-ring structure possessing larger tension, so it has a relatively higher thermal stability.

(b) The temperature range of thermal degradation ΔT is equal to the difference of the peak temperatures and the onset temperatures of degradation. COCs have narrower temperature ranges
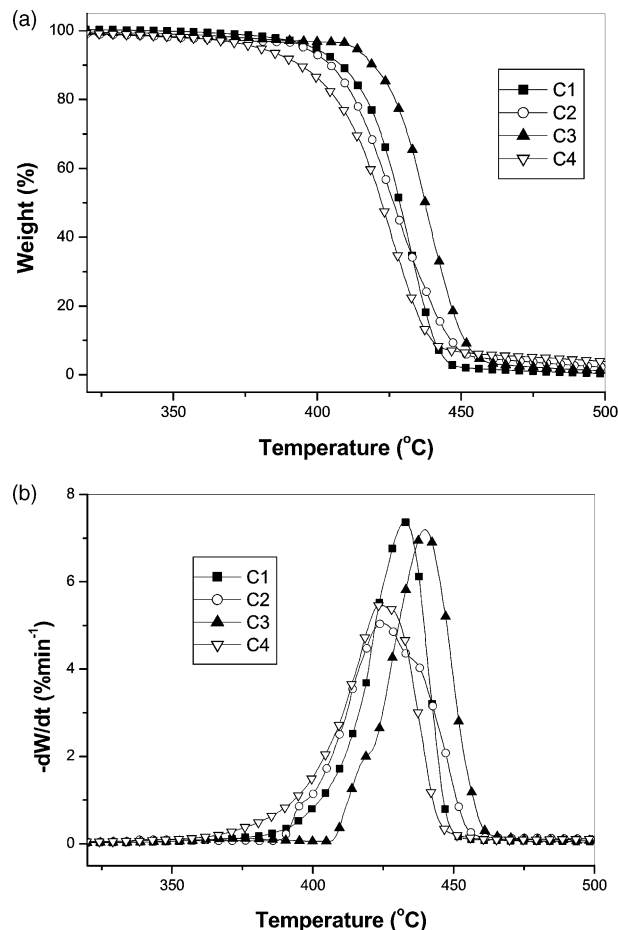

Fig. 3. The TGA curves (a) and DTG curves (b) of C-series COCs samples at heating rate 2 °C/min.

Table 2
Characteristic temperatures and activation energies obtained by the Flynn–Wall–Ozawa method for the COCs degradation

Sample	Onset temperature, T_{onset} (°C)	Peak temperature, T_p (°C)	ΔT^a (°C)	E_a at 50% conversion (kJ/mol)	$\Delta T_p{}^b$ (°C)
A1	412	432	20	200	33
A2	422	438	16	252	28
A3	417	435	18	229	30
A4	419	435	16	212	32
B1	413	432	19	189	36
B2	416	433	17	193	33
B3	417	435	18	201	32
C1	415	432	17	220	29
C2	407	424	17	154	48
C3	424	440	16	243	30
C4	404	424	20	165	43
HDPE	423	451	28	205	29

[a] ΔT—The difference of T_p and T_{onset}.
[b] ΔT_p—The shift of T_p at different heating rates (2 and 10 °C/min).

of degradation than HDPE, which means the chain scission happens in shorter time. Another effect of branching is a possible change of the reaction mechanism, therefore, the bonds next to a side chain exhibit a higher breakage rate than do normal PE bonds, which lead to a more pronounced maximum in the conversion rate curve.

(c) Because polyolefins consist of carbon and hydrogen elements, there is usually little or no residue once the degradation of polyolefin had ended. However, from Figs. 1(a), 2(a) and 3(a), it can be see that COCs have 2–5% black residual ash upon the end temperature of degradation, especially for samples with polar side-groups such as C2, C4. It is probably due to some crosslinked structures formed from the reaction between radicals. The rate of formed radicals increases with their stability, and therefore, the content of the crosslinked structures is higher if the radicals formed during the pyrolysis process are more stable. It needs more experimental work to determine the mechanism by which the residue is formed.
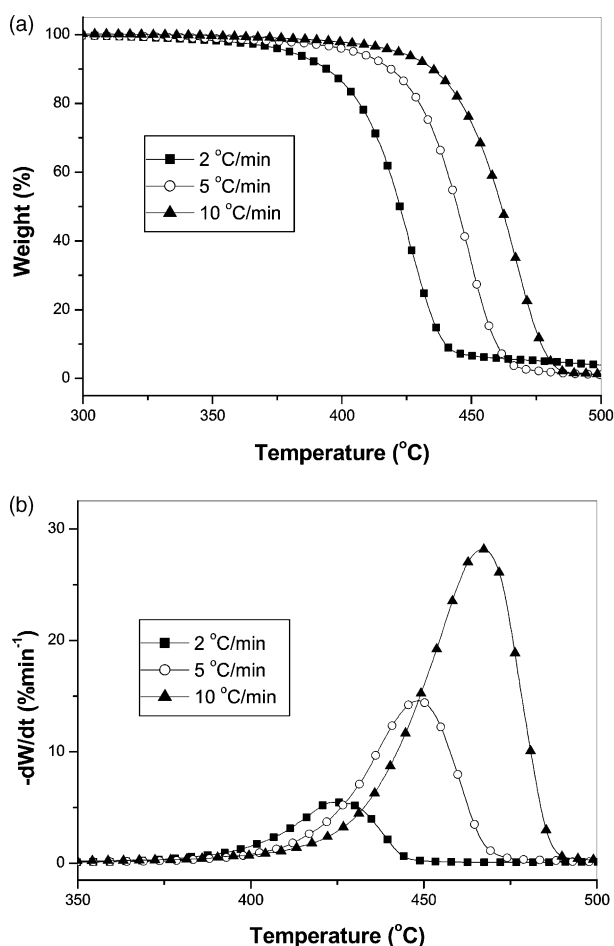
Fig. 4. The TGA curves (a) and DTG curves (b) of C4 sample at heating rates 2, 5 and 10 °C/min.

3.2. Kinetic evaluations

3.2.1. Multiple constant heating rates: Flynn–Wall–Ozawa method

Flynn and co-workers [35–37] derived a method for the determination of activation energy based on the equation:

$$\log\beta \cong 0.457\left(-\frac{E_a}{RT}\right) + \left[\log\left(\frac{AE_a}{R}\right) - \log F(\alpha) - 2.315\right] \quad (1)$$

where β is the heating rate, T is the absolute temperature, R is the gas constant, α is the conversion, E_a is the activation energy of the reaction, A is the pre-exponential factor. Thus, at the same conversion, the activation energy E_a is then obtained from the slope of the plot of $\log\beta$ against $1/T$.

Non-isothermal TGA of the sample was performed at constant heating rates of 2, 5 and 10 °C/min. The TGA and DTG curves for the pyrolysis of a typical sample C4 at different heating rates are shown in Fig. 4. It is clearly observed from these figures that the thermograms shift towards higher temperatures as the heating rate increases. This shift of thermograms to higher temperature with increasing β is expected and is due to a shorter time required for a sample to reach a given temperature at a faster heating rate. The values of the shift in the peak temperatures (ΔT_p) of different heating rates (2 and 10 °C/min) are listed in Table 2.

By using Eq. (1), the $\log\beta$ versus $-1/RT$ plots from 5 to 90% conversion for the degradation of C4 are shown in Fig. 5. The lines at different conversion values are approximately parallel to each other and all the correlation coefficients of linearity in calculation of each activation energy were larger than 0.98. Moreover, the activation energies of degradation calculated from these plots are shown in Fig. 6. It is evident that the activation
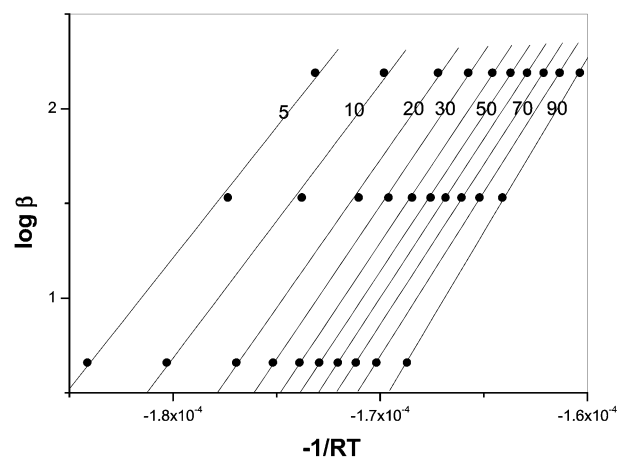
Fig. 5. Application of Flynn–Wall–Ozawa method for C4 at heating rates 2, 5 and 10 °C/min and conversions of 5, 10, 20, 30, 40, 50, 60, 70, 80, and 90%.
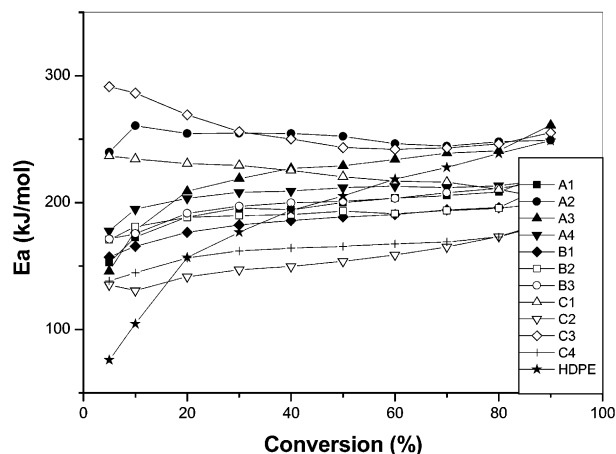
Fig. 6. Activation energies calculated as a function of conversion for COCs using the Flynn–Wall–Ozawa method.

Fig. 7. Pseudo first-order kinetic plot for C4 at heating rate 2 °C/min.

energies of degradation for these samples remain relatively constant after 10% conversion, which reveals that up to 10% conversion there is one dominant kinetic process. In contrast, the activation energy of HDPE increases with increasing conversion, which is similar to the values reported in literature [31,38].

The values of the activation energies of degradation at 50% conversion are listed in Table 2. However, as same as the influence of cyclic structure on the peak temperature, there is no clear trend between the activation energy of degradation and the cyclic structure content of these samples. The activation energy values for COCs are ±50 kJ/mol of that of HDPE, and are comparable with those of EPDMs [31]. The activation energy values 154 and 165 kJ/mol for C2 and C4 are somewhat lower than the value of HDPE, but is similar to the value of 170 kJ/mol for PS [39,40]. Lower values of E_a for C2 and C4 should be attributed to the increasing stability of the radicals formed during the pyrolysis process. On the other hand, A2 and C3 have higher E_a values 252 and 243 kJ/mol than other samples, which is consistent with their higher thermal stability.

3.2.2. Single heating rate: pseudo first-order method

For a first order reaction, Chan and Balke [41] have proved that the activation energy, E_a, is related to the weight fraction remaining in TGA run, W, the rate of weight loss, $-dW/dt$, and the temperature, T, by the following equation:

$$\ln\left(\frac{-dW/dt}{W}\right) = E_a\left(-\frac{1}{RT}\right) + \ln A \tag{2}$$

Therefore, for a first order degradation process, a plot of $\ln[(-dW/dt)/W]$ versus $[-1/(RT)]$ will be a straight line with slope equal to the activation energy E_a. The method is also useful for dealing with a change in mechanism if only a few values of activation energy will explain most of the data.
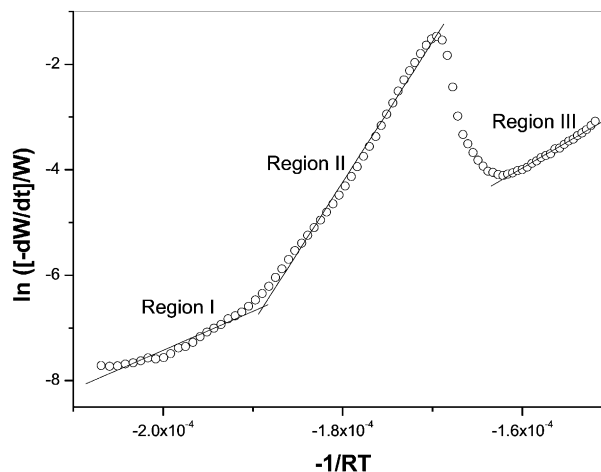
The reaction order of the non-isothermal degradation process, n, has been determined by the Kissinger method [42]:

$$n = 1.26\sqrt{s} \tag{3}$$

where s is the shape index of the differential thermal analysis curve for non-isothermal dynamic degradation. The shape index is the absolute value of ratio of slopes of tangents to the DTG curve at the inflection point, T_M. The reaction orders for degradations for COCs and HDPE are shown in Table 3.

The reaction order of HDPE is similar to the reported values in the literature [39,40], and the reaction orders of COCs are very close to 1, therefore, it is reasonable to assume the degradation reactions are all first order. Fig. 7

Table 3
Kinetic parameters for the degradation of COCs calculated using the pseudo-first order method at 2 °C/min

Sample	n[a]	Region I		Region II		Region III	
		$\ln A$ (min^{-1})	E_a (kJ/mol)	$\ln A$ (min^{-1})	E_a (kJ/mol)	$\ln A$ (min^{-1})	E_a (kJ/mol)
A1	0.95	21.2	146	53.8	327	10.6	90
A2	0.87	21.6	154	74.4	449	12.6	96
A3	0.96	13.8	109	53.7	346	10.5	91
A4	0.92	13.1	107	60.1	364	8.1	71
B1	0.90	7.4	74	59.2	358	14.8	113
B2	0.88	11.7	100	62.6	378	19.8	141
B3	0.88	10.4	92	59.0	358	18.0	130
C1	0.98	16.7	125	61.3	369	13.1	99
C2	1.03	7.7	76	42.0	259	7.7	69
C3	1.02	12.8	105	68.7	418	5.4	53
C4	0.92	14.0	108	46.5	282	12.6	104
HDPE	0.77	13.0	101	51.3	320	nd[b]	nd

[a] n—order of decomposition reaction as determined by the Kissinger method.
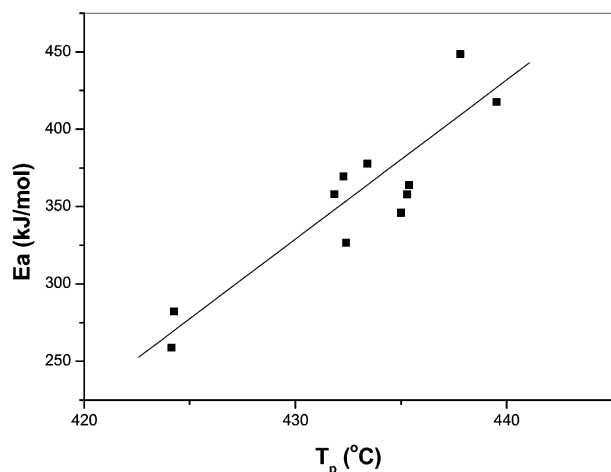
Fig. 8. Plot of E_a in Region II versus T_p at heating rate 2 °C/min.

shows a typical plot of $\ln[-\mathrm{d}W/\mathrm{d}t)/W]$ plotted against $-1/(RT)$ for a heating rate of 2 °C/min for sample C4. On the basis of Eq. (2), if the reaction were first order, we would have expected that these data could be fit by a straight line of slope equal to the activation energy.

Instead, in the figure three linear regions are observed, then three straight lines are needed to fit these data points. These regression lines, shown as solid lines in the figure, can be considered as three pseudo-first order regions and are designated as region I, region II and region III, respectively, with two transition zones between them. This observation indicates that three distinctly different types of reactions have dominated the degradation process. Similar results were obtained for all COCs samples, and a summary of the kinetic parameters obtained using the pseudo-first order method, shown in Table 3.

Chan et al. [41] and Gamlin et al. [31] have evaluated the kinetic parameters of degradation using the pseudo first-order method for PP and EPDM, respectively. There were two stages of degradation: the one at lower degradation temperatures was attributed to scission of 'weak links' [43] in the polymer; the other at higher temperatures was associated with random scission throughout the polymer. It is obvious that there are three different types of reactions dominating the COCs degradation process, instead of two types of reactions reported in the literature. The first two regions are
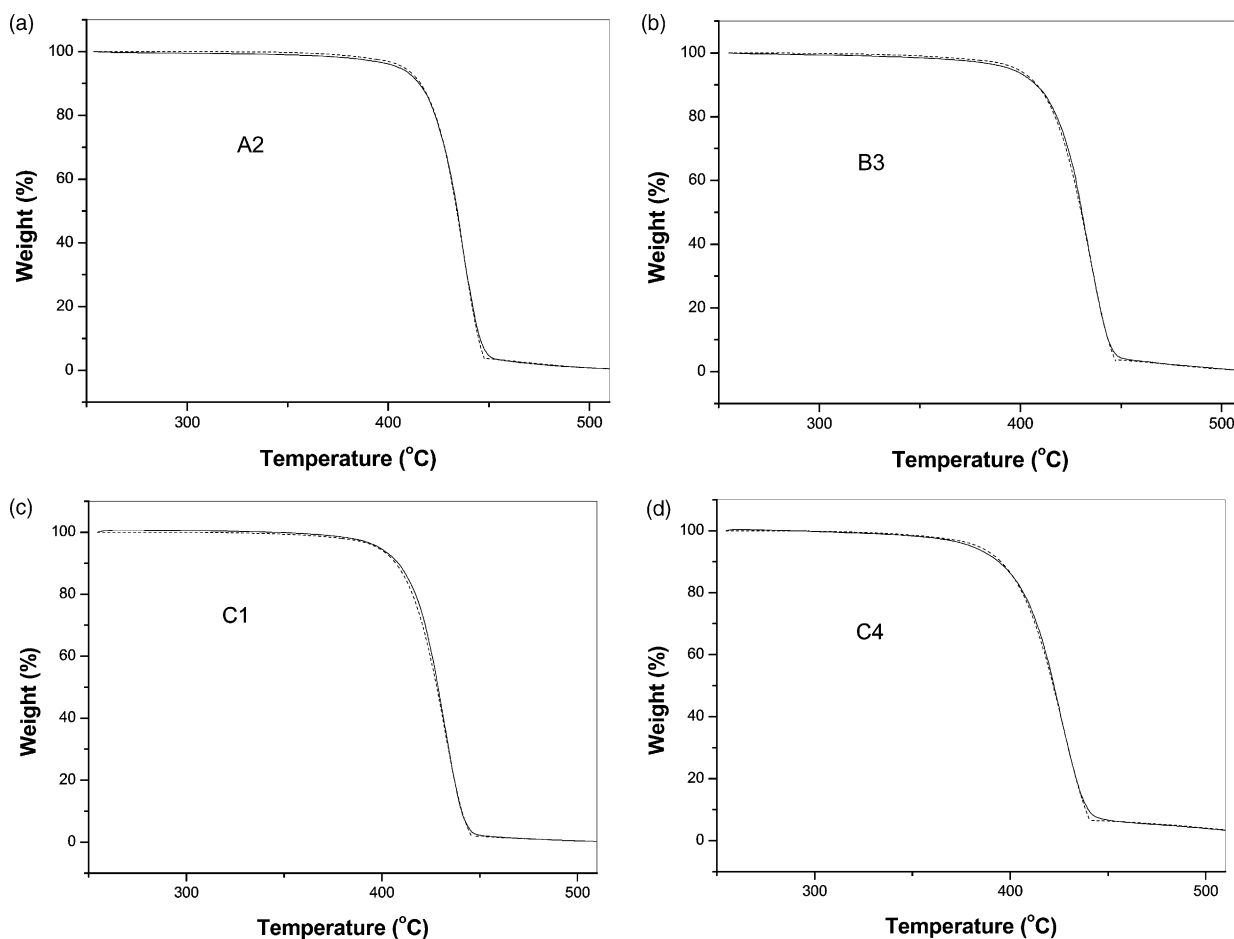

Fig. 9. Comparison between the experimental TGA curve and the curve calculated using the pseudo first-order kinetic parameters for A2 (a), B3 (b), C1 (c) and C4 (d) at heating rate 2 °C/min (— expt.; - - - model).

similar to region I and region II in the literature, but the region III that occurs upon conversion of 95%, it is postulated, is attributed to the degradation of the crosslinked structure. In Section 3.2, it has been provided that COCs have small amount of residual weight upon the end temperature of degradation. Abou-Shaaban et al. reported that crosslinked polyethylenes have three stages of degradation and the last one was attributed to the destruction of a graphite char from the crosslinked material [44].

The second difference between this work and the literature is the range of these regions. Region I extends from zero to around 15–30% conversions for PP and EDPM. However, for all COCs region I occurs under 5% conversion and region II covers a conversion range of approximately 5–95%. The shift of the location of transition region to lower conversion should be attributed to the structure features of COCs.

It should be noted that the activation energies in region II, calculated by using the pseudo first-order method, are much higher than those calculated by using the Flynn–Wall–Ozawa method. This phenomenon was observed for the degradations of PP and EPDM [31,41], and it was attributed that region II was characterized by large weight losses associated with high temperature and high degrees of chain scission. Recently, Yang et al. [45] reported the activation energy of the mCOC polymer was 349 kJ/mol on primary weight-loss region, which is consistent with the results in region II. In the present work, although the values of E_a in region II are higher, there is a similar change trend of E_a between two methods. However, it is surprising that the E_a in region II is proportional to the peak temperature of degradation for COCs, as shown Fig. 8. It seems that there is a good correlation between the degradation temperature and the activation energy for COCs.

As a check on the validity of the fit using the pseudo first-order method, theoretical weight loss versus temperature curves were generated by using the kinetic parameters E_a and A given in Table 3 for the three regions by using Eq. (4) [41]:

$$- \ln(1 - \alpha) = -\ln W = \frac{ART^2}{\beta E_a}\left(1 - \frac{2RT}{E_a}\right)\exp\left(-\frac{E_a}{RT}\right)$$
(4)

The TGA experimental curves and the predicted ones from the application of Eq. (4) are shown in Fig. 9 for samples A2, B3, C1 and C4 as representations of three-series COCs. As can be seen, a good overall fit is obtained for all four representations. However, in each case, slight deviations are noticeable near the transition ranges between regions. This is expected since the transition regions are not taken into account and the kinetic parameters vary significantly in this region. These results indicate that the analysis method used in this work is valid.

4. Conclusions

The thermal stability and degradation kinetics of three-series cyclic olefin copolymers have been reported in this research. Kinetic parameters of degradation were evaluated by using the Flynn–Wall–Ozawa *iso*-conversional method and the pseudo first-order method. It can be see that COCs have maintained the superior thermal stability of polyolefin materials, but COCs have lower peak temperatures of degradation, narrower degradation temperature ranges and higher amount of residual weights at the end of the degradation, which should be attributed to the chemical structure and microstructure features of COCs including the branching effect and the steric effect.

From the non-isothermal degradation dada, the kinetic parameters such as E_a and A for all the polymers have been calculated by using the methods of Flynn–Wall–Ozawa and the pseudo first-order. The values of the reaction order of COCs determined by the Kissinger method are close to 1, which verify the validity of the first-order assumption. There is no correlation between the calculated values for activation energy and the cyclic structure content of COCs in both methods, but there is a similar change trend of E_a between two different methods. However, the values of E_a in region II calculated by using the pseudo first-order method are much higher than those calculated by using the Flynn–Wall–Ozawa method. The E_a in region II is proportional to the peak temperature of degradation, which indicates that there is a good correlation between the degradation temperature and the activation energy for COCs. Finally, by using the estimated kinetic parameters, the predicted weight loss versus temperature curves well fit the experimental data, which supported the validity of estimated parameters and applicability of the analysis method used in this work.

References

[1] Schut JH. Plast Tech 2000 March.
[2] Lamonte RR, McNally D. Adv Mater Process 2001;159(3):33.
[3] Kaminsky W, Bark A, Arndt M. Makromol Chem Macromol Symp 1991;47:83.
[4] Kaminsky W. Adv Catal 2002;46:89.
[5] Imanish Y, Naga N. Prog Polym Sci 2001;26:1147.
[6] Bergström CH, Sperlich BR, Ruotoistenmäki J, Seppälä JV. J Polym Sci, Part A: Polym Chem 1998;36:1633.

[7] Ruchatz D, Fink G. Macromolecules 1998;31:4674.

[8] Arndt M, Beulich I. Macromolecules 1999;32:7335.

[9] Tritto I, Marestin C, Boggioni L, Zetta L, Provasoli A, Ferro DR. Macromolecules 2000;33:8931.

[10] Forsyth JF, Perena JM, Benavente R, Perez E, Tritto I, Boggioni L, et al. Macromol Chem Phys 2001;202:614.

[11] Arndt M, Beulich I. Macromol Chem Phys 1998;199:1221.

[12] Ruchatz D, Fink G. Macromolecules 1998;31:681.

[13] Rishe T, Waddon AJ, Dickinson LC, MacKnight WJ. Macromolecules 1998;31:1871.

[14] Forsyth JF, Scrivani T, Benavente R, Marestin C, Perena JM. J Appl Polym Sci 2001;82:2159.

[15] Shin JY, Park JY, Liu CY, He JS, Kim SC [in preparation].

[16] Scrivani T, Benavente R, Perez E, Perena JM. Macromol Chem Phys 2001;202:2547.

[17] Chu PP, Huang W-J, Chang F-C, Fan SY. Polymer 2000; 41:401.

[18] Chu PP, Cheng M-H, Huang W-J, Chang F-C. Macromolecules 2000;33:9360.

[19] DorKenoo K, Pfromm PH, Rezac ME. J Polym Sci, Part B: Polym Phys 1998;36:797.

[20] DorKenoo K, Pfromm PH. J Polym Sci, Part B: Polym Phys 1999;37:2239.

[21] Khanarian G. Opt Eng 2001;40:1024.

[22] Khanarian G. Polym Eng Sci 2000;40:2590.

[23] Delfolie C, Dickinson LC, Freed KF, Dudowicz J, MacKnight WJ. Macromolecules 1999;32:7781.

[24] Matti P, Okamoto M, Kotaka T. Polymer 2001;42:3939.

[25] Matti P, Okamoto M, Kotaka T. Polymer 2001;42:9827.

[26] Takigawa T, et al. Chem Int 2000; 22(5):142.

[27] Kaminsky W, Benlich I, Arndt M. Macromol Symp 2001; 173:211.

[28] Chem Int 2000;22(5).

[29] Westerhout R, Waanders J, Kuipers J, van Swaaji W. Ind Eng Chem Res 1997;36:1955.

[30] Morrison RT, Boyd RN. Organic chemistry. 2nd ed. Boston: Allyn and Bacon; 1966.

[31] Gamlin C, Dutta N, Choudhury NR, Kehoe D, Matisons J. Thermochim Acta 2001;367-368:185.

[32] Stivala SS, Kimura J, Gabbay SM. In: Allen NS, editor. Degradation and stabilization of polyolefins. New York: Applied Science Publishers; 1983. p. 101.

[33] Zuev VV, Brtini F, Audisio G. Polym Degrad Stab 2001;71:213.

[34] De P, Chattopadhyay S, Madras G, Sathyanarayana DN. Polym Degrad Stab 2002;76:511.

[35] Flynn JH, Wall LA. Polym Lett 1966;4:323.

[36] Ozawa T. Bull Chem Soc Jpn 1965;38:1881.

[37] Ozawa T. J Therm Anal 1970;2:301.

[38] Anderson DA, Freeman ES. J Polym Sci 1961;54:253.

[39] Wu CH, Chang CY, Hor JL. Waste Management 1993;13:221.

[40] Yang J, Miranda R, Roy C. Polym Degrad Stab 2001;73:455.

[41] Chan JH, Balke ST. Polym Degrad Stab 1997;57:135.

[42] Kissinger HHE. Anal Chem 1957;29:1702.

[43] Jellinek HHG. J Polym Sci 1948;3:850.

[44] Abou-Shaaban RRA, Haberfled JL, Barrall EM, Johnson JF, Simonnelli AP. Polym Eng Sci 1976;16:544.

[45] Yang TCK, Lin SSY, Chuang TH. Polym Degrad Stab 2002; 78:525.